4^{th} *URSI AT-RASC, Gran Canaria, 19 – 24 May 2024*

TE-wave propagation in a circular waveguide with impedance-matched RHM to LHM transition

Mariana Dalarsson*(1), Mika Söderström(1), and Balwan Rana(1)
(1) Department of Electrical Engineering, School of Electrical Engineering and Computer Science, KTH Royal Instiitute of Technology, 100 44 Stockholm, Sweden.
e-mail: mardal@kth.se

Abstract

We study TE-wave propagation in a circular waveguide with a graded transition from a lossy right-handed material (RHM) filling the left-hand half of the waveguide to the impedance-matched lossy left-handed material (LHM) filling the right-hand half of the waveguide. We obtain exact analytical solutions to Maxwell's equations and perform corresponding numerical simulations in COMSOL. An excellent agreement is obtained between the numerical simulations and analytical results. The presented method can model smooth realistic material transitions, where the interface width is an additional degree of freedom in the design of practical RHM-LHM interfaces.

1 Introduction

Graded material composites are of interest in several areas. In transformation optics (TO), metamaterials with spatially dependent material parameters are used to manipulate the propagation of waves [1] in optical devices such as flat lenses or reflectionless beam bends. A graded refractive index (GRIN) material for a thin-film solar cell structure has been shown to suppress the reflections [2]. GRIN lenses have been studied in medical applications to monitor the neural brain activity in relation to substance use disorders [3]. GRIN materials have also been used in waveguides where higher bandwidth and lower losses was achieved, compared to discrete material transitions [4]. Yet another example of GRIN materials used in waveguides to control the effect of transmission or design bending waveguide structures without destroying the field pattern was presented in [5].

Following the approach employed in our previous work like e.g. [6], in the present paper, we consider a new problem of the TE-wave propagation in a hollow circular waveguide containing a metamaterial composite consisting of a right-handed material (RHM) and left-handed material (LHM). The transition between the materials is graded according to a hyperbolic tangent function in the direction of propagation [6]. The objective is to find the exact analytical solutions for the fields of arbitrary order TE-modes in a circular waveguide. The analytical results are then compared to the corresponding numerical simulation results, obtained using COMSOL Multiphysics, for the lowest order TE_{11} mode. Thereby, we confirm an excellent agreement between the analytical results and corresponding numerical simulations.

2 Analytical results

Consider a hollow circular waveguide with radius a and length L along the z-axis, as shown in Figure 1.

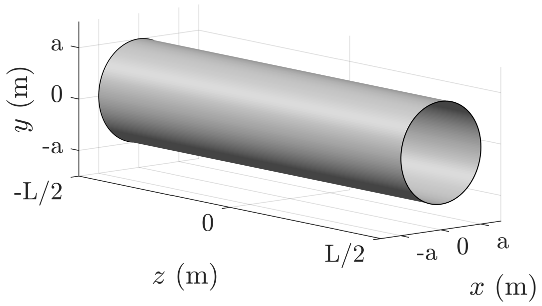

Figure 1. Circular waveguide with radius a and length L.

The time convention $e^{i\omega t}$ is used for time-harmonic fields, and the spatially varying permeability and permittivity are defined as continuous functions of z as follows [6]

$$\mu(z) = -\mu_0 \frac{\mu_{I1}+\mu_{I2}}{2\beta}\left(\tanh\frac{z}{z_0} + i\beta\right) \tag{1}$$

$$\varepsilon(z) = -\varepsilon_0 \frac{\varepsilon_{I1}+\varepsilon_{I2}}{2\beta}\left(\tanh\frac{z}{z_0} + i\beta\right) \tag{2}$$

where the explicit ω-dependence of the permeability and permittivity parameters is dropped for the sake of brevity. From e.g. [6] we recall the impedance-matching condition

$$\beta = \frac{\varepsilon_{I1}+\varepsilon_{I2}}{2\varepsilon_R - i(\varepsilon_{I1}-\varepsilon_{I2})} = \frac{\mu_{I1}+\mu_{I2}}{2\mu_R - i(\mu_{I1}-\mu_{I2})} \tag{3}$$

For $z \to -\infty$, in the RHM-material, we have $\varepsilon_1(\omega,z) = \varepsilon_0(+\varepsilon_R - i\varepsilon_{I1})$ and $\mu_1(\omega,z) = \mu_0(+\mu_R - i\mu_{I1})$, while for $z \to +\infty$, in the LHM-material, we have $\varepsilon_2(\omega,z) = \varepsilon_0(-\varepsilon_R - i\varepsilon_{I2})$ and $\mu_2(\omega,z) = \mu_0(-\mu_R - i\mu_{I2})$, as required for impedance-matched passive materials. The electric field $\boldsymbol{E} = \boldsymbol{E}_T = E_r\,\hat{\boldsymbol{r}} + E_\varphi\,\hat{\boldsymbol{\varphi}}$ for TE-modes satisfies the equation

$$\nabla^2\boldsymbol{E} - \frac{1}{\mu}\frac{d\mu}{dz}\frac{\partial\boldsymbol{E}}{\partial z} + k^2(z)\,\boldsymbol{E} = 0 \tag{4}$$

where $k^2(z) = \omega^2\varepsilon(z)\mu(z)$ is the square of the wavenumber in the medium. The two components of the solution to this equation in cylindrical coordinates (r, φ, z) are

$$E_r(r,\varphi,z) = \frac{\mathrm{i}\omega H_0}{k_t^2}\frac{n}{r} J_n\left(x'_{mn}\frac{r}{a}\right)\cos(n\varphi)\mathrm{e}^{-\mathrm{i}I(z)} \quad (5)$$

$$E_\varphi(r,\varphi,z) = -\frac{\mathrm{i}\omega H_0}{k_t^2}\frac{x'_{mn}}{a} J'_n\left(x'_{mn}\frac{r}{a}\right)\sin(n\varphi)\mathrm{e}^{-\mathrm{i}I(z)} \quad (6)$$

where H_0 is a constant with the dimension of magnetic field strength [A/m]. The transverse wave number k_t is given by $k_{tmn} = x'_{mn}/a$ with x'_{mn} being the m-th zero of the first derivative of the n-th order Bessel function $J_n(x)$, so that $J'_n(x'_{mn}) = 0$. The z-dependent function $I(z)$ is

$$\begin{aligned} I(z) = \frac{\kappa z_0}{2}\Bigg\{ &\sqrt{w^2(z)+2aw(z)+L} + \sqrt{L}\,\ln w(z) \\ &+ a\,\ln\left[a + w(z) + \sqrt{w^2(z)+2aw(z)+L}\right] \\ &-\sqrt{L}\ln\left[L + aw(z) + \sqrt{L}\sqrt{w^2(z)+2aw(z)+L}\right] \\ &+\sqrt{u^2(z)+2bu(z)+M} + \sqrt{M}\,\ln u(z) \\ &+ b\,\ln\left[b + u(z) + \sqrt{u^2(z)+2bu(z)+M}\right] \\ &-\sqrt{M}\ln\left[M + bu(z) + \sqrt{M}\sqrt{u^2(z)+2bu(z)+M}\right]\Bigg\} \end{aligned} \quad (7)$$

where $a = 1+\mathrm{i}\beta$, $b = 1-\mathrm{i}\beta$ and

$$\begin{Bmatrix} u(z) \\ w(z) \end{Bmatrix} = 1 \pm \tanh\frac{z}{z_0}\ , \quad \begin{Bmatrix} L \\ M \end{Bmatrix} = (1\pm\mathrm{i}\beta)^2 - \frac{k_t^2}{\kappa^2} \quad (8)$$

with the constant κ defined by

$$\kappa^2 = \omega^2\varepsilon_0\mu_0\frac{\varepsilon_{I1}+\varepsilon_{I2}}{2\beta}\frac{\mu_{I1}+\mu_{I2}}{2\beta} \quad (9)$$

Asymptotically, the function $I(z)$ becomes $I(z) \to k_z(\pm\infty)z$, where $k_z^2(z) = k^2(z) - k_t^2$, as expected in RHM and LHM materials, respectively. The z-dependency of the material parameters does not affect the transverse parts of the field components, which can be recognized as the well known textbook solutions for a circular waveguide.

3 Numerical simulation in COMSOL

The numerical simulations are performed with COMSOL Multiphysics software. A hollow cylindrical waveguide with perfectly conductive walls, radius a and length L, is set up along the z-axis. The waveguide is filled by the graded metamaterial composite with RHM filling the left-hand side of the waveguide, and LHM filling the right-hand side of the waveguide, as shown in Figure 2.

A TE_{11} wave is excited from the port connected to the left-hand side of the waveguide. At both ends of the structure, two cylindrical boxes of perfectly matched layers (PMLs) are added together with scattering boundary conditions at the very ends of the PMLs. This ensures that any waves outside the ports are absorbed and not scattered back into the structure.

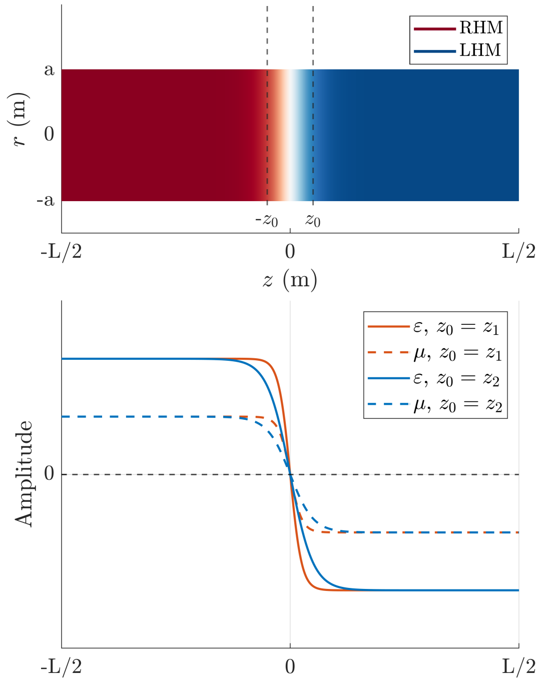

Figure 2. Graded RHM-LHM material along the z-axis in the waveguide.

4 Comparison and discussion

A comparison between analytical and numerical results for the wave propagation of the TE_{11}-mode ($m = 1$ and $n = 1$), is performed for a circular waveguide with radius $a = 0.5$ m and length $L = 2$ m. In this case, we have $x'_{mn} = 1.8412$. The material parameters are chosen to be $\varepsilon_{RHM} = 2 - \mathrm{i}\,0.04$, $\mu_{RHM} = 1 - \mathrm{i}\,0.02$ in RHM, as well as $\varepsilon_{LHM} = -2 - \mathrm{i}\,0.02$, $\mu_{LHM} = -1 - \mathrm{i}\,0.01$ in LHM. Two lengths of the transition region, $z_0 = 0.01$ m, and $z_0 = 0.04$ m are considered. The operating frequency is chosen to be 1 GHz.

4.1 Longitudinal field pattern

The longitudinal pattern of the electric field along the structure has been evaluated by studying the normalized electric field intensity $E(a/2, 0, z)$. The comparison between the analytical and numerical results for $z_0 = 0.01$ is shown in Figure 3 (a), while the comparison between the analytical and numerical results for $z_0 = 0.04$ is shown in Figure 3 (b). From Figure 3, we see an excellent agreement between the analytical and numerical results. We see that the direction of the wave vector is changed at $z = 0$, where the transition from RHM to LHM occurs, as expected.

4.2 Transversal field pattern

The transversal distribution pattern of the field is independent of the position in the direction of wave propagation (z-direction), even though we have a material variation in z-direction. The electric field patterns at $z = -L/2$ and $z = L/2$ are shown in Figures 4 (a) and 4 (b), respectively.

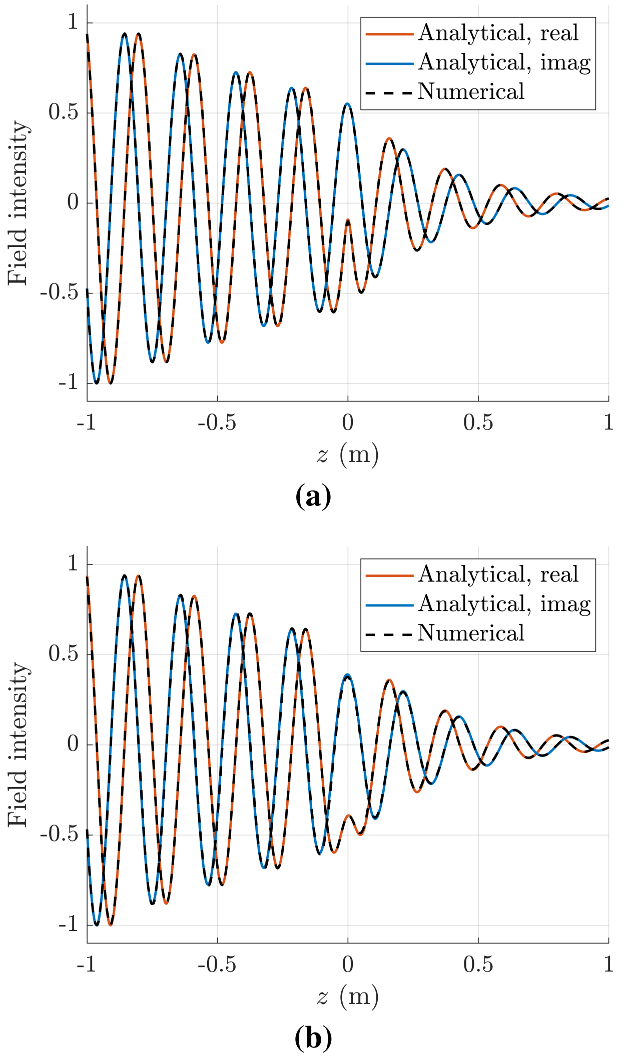

Figure 3. A comparison of the analytical and numerical results for two different lengts of the transition region of (a) $z_0 = 0.01$ m, and (b) $z_0 = 0.04$ m.

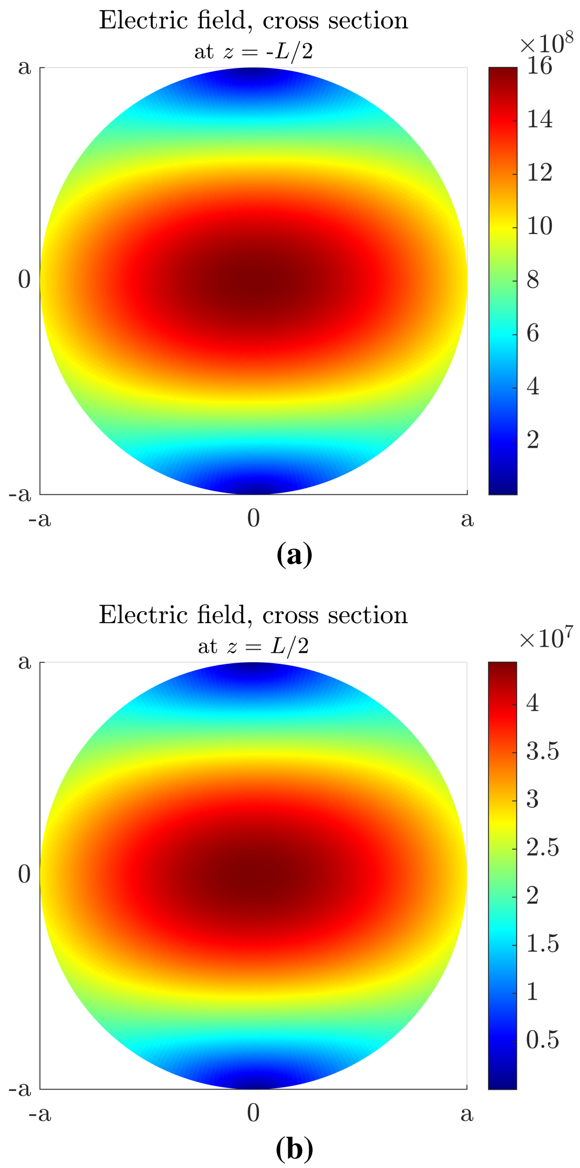

Figure 4. Transversal electric field intensity pattern at (a) $z = -L/2$ and (b) $z = L/2$. In both figures, the transition region length is $z_0 = 0.01$ m.

The two field patterns are the same, as expected. The field magnitudes at the two longitudinal positions are, however, not equal to each other, due to the attenuation of the wave throughout the waveguide. The analytical results for the transversal electrical field components are also in excellent agreement with the corresponding results obtained using numerical simulations in COMSOL.

5 Conclusions

In this paper, TE-wave propagation in a circular waveguide filled by a metamaterial composite with a graded transition between RHM and LHM, is studied both analytically and numerically. The analytical solution of Maxwell's equations is in excellent agreement with the numerical results obtained in COMSOL, both for the transverse and for the longitudinal parts of the field intensity along the structure. The results are also in agreement with the expected behavior of wave propagation in a graded RHM-LHM composite. The presented results also show that it is possible to perform accurate numerical simulations on these structures. This is of importance for future studies where both exact analytical analysis as well as numerical simulations can be used to study and design GRIN waveguide devices.

6 Acknowledgements

The work of M. D. was supported by the Swedish Research Council, project number 2018-05001.

References

[1] Q. Wu, J. P. Turpin, and D. H. Werner, "Integrated photonic systems based on transformation optics enabled gradient index devices," Nature, Light: Science

Applications, vol. 1, pp. 1–6 (2012).
DOI: 10.1038/lsa.2012.38.

[2] S. J. Jang, Y. M. Song, C. I. Yeo, C. Y. P. J. S. Yu, and Y. T. Lee, "Antireflective property of thin film a-si solar cell structures with graded refractive index structure," Optics Express, vol. 19, pp. 108–117 (2011). DOI: 10.1364/OE.19.00A108.

[3] N. J. Beacher, K. A. Washington, Y. Zhang, Y. Li, and D.-T. Lin, "Grin lens applications for studying neurobiology of substance use disorder," Addiction Neuroscience, vol. 4, p. 100 049 (2022).
DOI: 10.1016/j.addicn.2022. 100049.

[4] J. Missinne, L. Misseeuw, X. Liu,et al., "Planar polymer waveguides with a graded-index profile resulting from intermixing of methacrylates in closed microchannels," Optical Materials, vol. 76, pp. 210–215 (2018). DOI: 10.1016/j.optmat.2017.12.039.

[5] Y. Fu, Y. Xu, and H. Chen, "Applications of gradient index metamaterials in waveguides," Scientific Reports, vol. 5, pp. 1–6 (2015).
DOI: 10.1038/srep18223.

[6] B. Rana, B. B. Svendsen, and M. Dalarsson, "TEM-wave propagation in a coaxial waveguide with impedance-matched RHM to LHM transition,"
Optics Express 30(18), pp. 32610-32620 (2022).
DOI: 10.1364/OE.460924